Aging in complex interdependency networks

Dervis C. Vural,[1,*] Greg Morrison,[1,2] and L. Mahadevan[1,3,4,†]

[1]*School of Engineering and Applied Sciences, Harvard University, Cambridge, Massachusetts, USA*

[2]*Department of Economics, IMT Institute for Advanced Studies, Lucca 55100, Italy*

[3]*Department of Physics, Harvard University, Cambridge, Massachusetts, USA*

[4]*Department of Organismic and Evolutionary Biology, Harvard University, Cambridge, Massachusetts, USA*

(Received 9 April 2013; published 24 February 2014)

Although species longevity is subject to a diverse range of evolutionary forces, the mortality curves of a wide variety of organisms are rather similar. Here we argue that qualitative and quantitative features of aging can be reproduced by a simple model based on the interdependence of fault-prone agents on one other. In addition to fitting our theory to the empiric mortality curves of six very different organisms, we establish the dependence of lifetime and aging rate on initial conditions, damage and repair rate, and system size. We compare the size distributions of disease and death and see that they have qualitatively different properties. We show that aging patterns are independent of the details of interdependence network structure, which suggests that aging is a many-body effect, and that the qualitative and quantitative features of aging are *not* sensitively dependent on the details of dependency structure or its formation.

DOI: 10.1103/PhysRevE.89.022811 PACS number(s): 64.60.aq, 87.18.Vf, 87.23.Kg

I. INTRODUCTION

For a collection of s radioactive atoms, the probability of decay is a constant, so that the fraction of atoms that decays per unit time $-(ds/dt)/s = \mu$ does not change in time. In other words, an old atom is equally likely to decay as a young one. Contrastingly, in complex structures such as organizations, organisms, and machines, one finds that the relative fraction that dies per unit time $\mu(t)$ varies, and typically increases in time. In living systems the mortality rate $\mu(t)$ increases exponentially (commonly known as the Gompertz law) up until a late-life plateau, after which aging decelerates. Moreover, the functional form of $\mu(t)$ for a wide variety of organisms is remarkably similar [1–3].

The origins of biological aging has been sought in two broad classes of nonexclusive theories [4,5]. The first, the mechanistic approach, aims to understand aging in terms of mechanical and biochemical processes such as telomere shortening [6] or reactive oxygen species damage [7]. The second approach considers aging as the outcome of evolutionary forces [8]. The early evolutionary theories are based on the observation that selective pressure is larger for traits that appear earlier in life [9–11]. As a result, aging, it has been argued, could be due to late-acting deleterious mutations accumulated over generations [mutation accumulation theory (MA)] [9,12] or due to mutations that increase fitness early in life at the cost of decreasing fitness later in life [antagonistic pleiotropy theory (AP)] [10,13,14]. Physiological variants of AP consider the relative energy cost of avoiding aging damage versus reproducing [15,16]: Mutations diverting energy away from repair and maintenance activities to earlier sexual development and high reproduction rate can be favored.

These theories are not problem free. The neutral (i.e., nonselective, nondirectional) MA theory has two predictions: a monotonic increase in the mortality rate with age, and an increased variation (spread) in mortality rate among different polymorphisms with age, both of which disagree with observation [17–19]. The non-neutral (i.e., selective, directional) AP theory predicts that every aging gene comes with an early-life enhancement of fecundity. While some such genes have been found, others contradict this prediction [20–23].

Much like the historical development of an engineered technological device, the complexity of life appears to have irreversibly increased as a large number of individual components become linked through their specialized functions [24–27]. Here we argue that a long history of both selectively neutral or non-neutral evolution inevitably leads to a convoluted interdependence between components, and it is this interdependency that causes observed aging patterns in complex organisms. To this end, we construct random and nonrandom dependency networks to represent neutral and non-neutral evolutionary histories, subject both ensembles to damage and repair, determine $\mu(t)$, and compare the outcomes of our model with the empiric mortality rate of six different species. Our approach does not exclude earlier mechanistic and evolutionary theories, and can be interpreted using the language of either.

Our work combines ideas from the theory of constructive evolution [24–27], network theory [28–33] and reliability theory of aging [34,35]. Allowing us to go beyond static analysis of connectivity and study the dynamics of the deterioration of a dependence structure.

II. MODEL

To study the dynamics of aging quantitatively, we start with a simple view of an organism as a set of nodes with dependencies characterized by directed edges between them. Each node may be thought as genes in a regulatory network, or the differentiated cells or tissues in a multicellular organism

*dcvural@seas.harvard.edu

†lm@seas.harvard.edu

with specific functions. A directed edge from node A to node B indicates that A provides something to B such as energy, crucial enzymes, or mechanical support, so that the function of B relies on the function of A. In this scenario, the evolution of the network is represented by random addition of new nodes and edges, leading to a change in the dependency structure of the network. This then changes the susceptibility of the network to further changes, including its longevity.

The evolution of populations are governed by neutral and non-neutral processes that widen or skew phenotype distributions. If the formation of a dependency is selectively neutral [26], then a node can depend on any other node i with equal probability $\wp_i$, regardless of node degree k. Thus uniform $\wp_i = \text{const.}$ and nonuniform $\wp_i = k_i / \sum_j k_j$ node attachment probabilities can be interpreted as the outcomes of neutral and non-neutral evolutionary processes (see Refs. [26] and [36] for discussion and further empiric justification). These two processes yield two very different network topologies known as random (RN) and scale-free (SFN) networks.

The structure of networks is expected to influence the dynamics of any processes on it, including aging. However we surprisingly observe that the two very different processes for network growth lead to very similar average life spans and mortality curves.

For a given network, we assume that its dynamics are governed by three parameters and one initial condition: The failure rate $\gamma_0 \ll 1$ and repair rate $\gamma_1 \ll 1$ of individual nodes, total number of nodes $N \gg 1$, and the initial fraction of damaged nodes $d \ll 1$. γ_0 is controlled by biomolecular processes, which are the subject of mechanical theories of aging (e.g., oxidative stress, radiation damage); the damage due to prenatal or postnatal stress is contained in the initial condition d. γ_1 depends on the activity or inactivity of genes or their regulators that may be relevant for repair and replacement of cells. It seems difficult to determine or modulate N, though it should roughly correlate with the complexity of an organism.

We assume that the aging of complex dependency networks are governed by the following three rules: (i) Every component in the organism must depend on at least one other node, and at least one other node must depend on it (i.e., all parts of the organism must be fully connected). (ii) With certain fixed small probabilities the components can break (stop functioning) or be repaired (start functioning). (iii) A node stops functioning if the majority of those on which it depends (providers) stop functioning, and cannot be repaired without a majority of its providers functioning. We specifically implement these rules as follows:

(i) Create a network model of an organism

(a) Begin with a single node, and $i = 1$.

(b) Introduce a new $(i+1)$th node and make it depend on any one of the preexisting nodes $j \leqslant i$ with probability $P(k_j)$, where k_j is the degree of node j. For the neutral scheme $P(k_j)$ is taken to be uniform and independent of k_j, whereas for the non-neutral scheme $P(k_j)$ is taken proportional to k_j.

(c) Make any existing node j depend on the $(i+1)$th node with probability $P(k_j)$

(d) Increment i and repeat step (b) and (c) for $N-1$ steps.

(ii) Age the resulting network model of an organism

(a) Define the organism state $\vec{\psi}(t) = \{x_1(t), x_2(t), \ldots, x_N(t)\}$ where every component can take either one of the values 1 (functional) or 0 (nonfunctional). The vitality of the organism is defined as $\phi(t) = \Sigma_i x_i(t)/N$. Assign a value of 0 to a fraction d of randomly selected nodes and 1 to the rest, corresponding to the initial state of an organism.

(b) For all i, update $x_i = 1$ to $x_i = 0$ with probability γ_0, flip $x_i = 0$ to $x_i = 1$ with probability γ_1, and do nothing with probability $1 - \gamma_0 - \gamma_1$.

(c) Break a node if the majority of nodes on which it depends are broken. Recursively repeat until no additional node breaks.

(d) Set $\vec{\psi}(t+1)$ to the outcome of step (c).

(e) Increment t and repeat (b)–(d) until all nodes are broken [i.e., $\sum_i x_i(t) = 0$].

In order to study the network mortalities, we must define a time of death τ, for which we define a threshold $\eta = \phi(\tau) = 1\%$ below which an organism is defined dead [37]. Our outcomes are unaffected by this choice for large N [38].

To establish the statistical properties of mortality in our network, we generate an ensemble of networks (organisms) and age them according to the above rules. In addition to tracking the vitality of the network characterized by $\phi(t)$, we also determine the fraction of individuals (not components) $s(t)$ that remain alive at time t so that the time dependent mortality rate is

$$\mu(t) = -[s(t+1) - s(t)]/s(t). \tag{1}$$

We also track the strength of interdependence between nodes characterized by the ratio

$$\lambda[\phi(t)] = \log[\phi(t)]/\log[\phi_0(t)],$$

where $\phi_0 = \exp\{(-\gamma_0 + \gamma_1)t\}$ is the expectation value of the vitality of an identical size network with all dependency edges removed. In other words, λ quantifies how fast an interdependent system decays compared to an independent one, as a function of time.

Finally, to analyze the magnitudes of functionality loss we consider the probability distribution $S[\Delta\phi]$ of event sizes $\Delta\phi$ (i.e., changes in ϕ). Each event represents an individual disease or recovery, the final one of which is death.

III. RESULTS

Typically, an organism starts its life with a slow decay of live cells ϕ at a rate of $\langle a \rangle \gamma_0$, where the dimensionless number $\langle a \rangle = 1.80$ for scale-free networks and $\langle a \rangle = 1.75$ for random networks. As an increasing number of nodes die, the system approaches a critical vitality $\phi(\tau) = \phi_c$ when all live nodes suddenly collapse. Typical trajectories for both network topologies as well as the values of $\langle a \rangle$ and ϕ_c are shown in Fig. 1.

We observe that even if γ_1 is set equal to γ_0 the system decays steadily despite the seeming reversibility in dynamics. This is because while any live node can break, not all the dead nodes will have the sufficient number of live providers to sustain a repair.

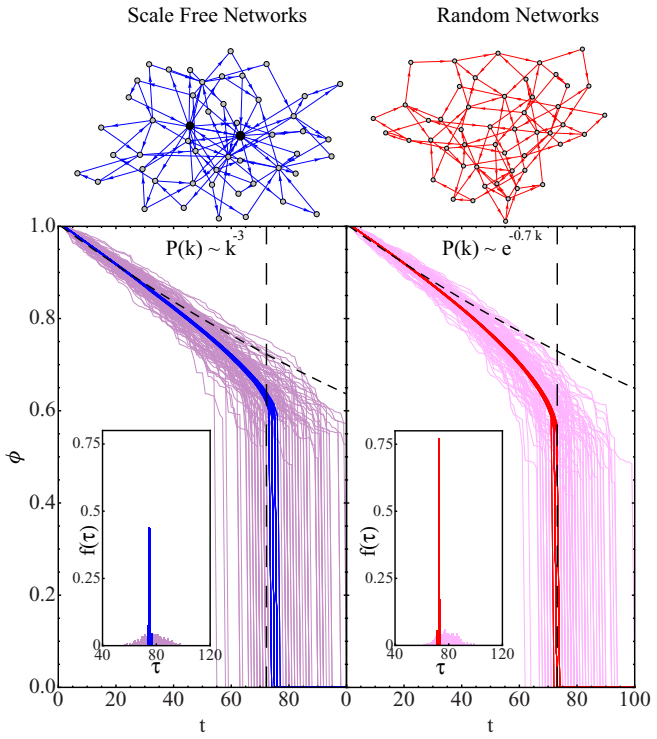

FIG. 1. (Color online) Fraction $\phi(t)$ of live nodes, 100 runs. Dependency structures grown via non-neutral (left column) and neutral (right column) evolutionary schemes yield scale-free (SFN) and random degree (RN) distributions $P(k)$. Although SFNs have high-degree hubs (black nodes) absent in RN, their aging characteristics share remarkable similarity. We plot 100 runs of $\phi(t)$ for each network size N and topology. Inset shows lifetime τ distributions $f(\tau)$. Increasing $N = 2500$ (light purple and pink) to $N = 10^6$ (dark blue and red) sharpens $f(\tau)$. The black lines mark our theoretical predictions for initial slope p_0 (=$1.80\gamma_0$ for SFN and =$1.75\gamma_0$ for RN) and critical fraction ϕ_c (=0.6 for SFN and =0.5 for RN), which agree well with simulations. Here $\{\gamma_0,\gamma_1,d\} = \{0.0025,0,0\}$.

In Fig. 2 we quantitatively compare the mortality curves generated by our digital populations to that of a variety of organisms, C. elegans, drosophila, medflies, beetles, mice, Himalayan goats (Tahr), using data compiled from [1–3], and see reasonable agreement between simulation and data.

To show that our parameters are individually relevant we fit the empirical mortality curves for a long-lived mutant and wild type of a fixed organism C. elegans. These two polymorphisms must have similar N values, and since they are subject to the same environmental conditions must be subject to similar kinds of damage and initial conditions. The difference between their mortality curves can be accounted for by fixing N,γ_0, and d constant while varying the repair rate γ_1 (Fig. 3). Since it is not possible to account for the difference by varying γ_0 while keeping the other parameters constant one can deduce that the enhanced longevity of the mutant must be due to higher repair metabolism rather than lower susceptibility to damage.

Since complex interdependency is not exclusive to living organisms, we also fit the empirical aging curves to our model of two kind of automobiles, the 1980 Toyota and 1980 Chevrolet obtained from Ref. [3] and find good agreement (Fig. 4).

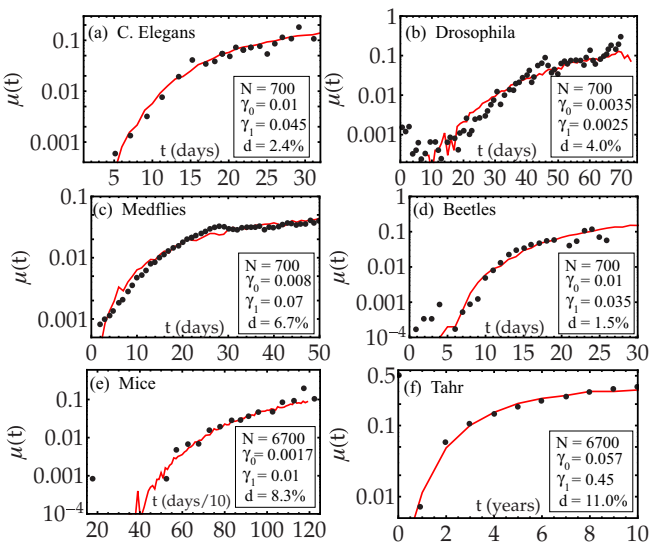

FIG. 2. (Color online) Empirical mortality data (black dots) fit to present theory (red lines). The mortality curves of (left to right) C. elegans, drosophila, medflies, beetles, mice, Himalayan goats from Refs. [1–3]. The horizontal axis and units of $1/\gamma_{0,1}$ is time in units of days for C. elegans, drosophila, medflies, and beetles; days/10 for mice and years for tahr. Varying three of the four parameters (N, $\gamma 1$ and d) simultaneously produces similar $\mu(t)$ curves (cf. Appendix); therefore we fix N (arbitrarily) and fit the remaining three parameters.

The effects of the system parameters on the mortality rate for both scale-free and random networks can be summarized as follows (Fig. 5): Increasing γ_0 shifts $\mu(t)$ left; increasing γ_1 decreases the value of $\mu_0 = \mu(t \to \infty)$ at the late-life plateau; increasing N increases the slope of μ in the aging (Gompertz) regime; in other words, larger systems age rapidly and suddenly, while small systems with few component systems are virtually nonaging. Increasing the initial damage d simply

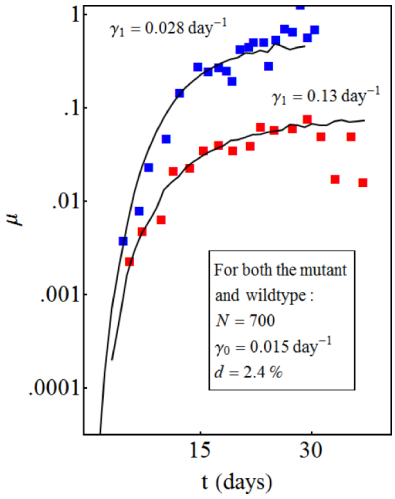

FIG. 3. (Color online) Mortality rate of mutant and wild-type nematodes. We fit the data (square markers) from Fig. 3E of Ref. [3] using our model (solid lines). To demonstrate that our model parameters have individual relevance we fit the mortality curves of a wild-type and long-lived mutant by only altering the repair rate.

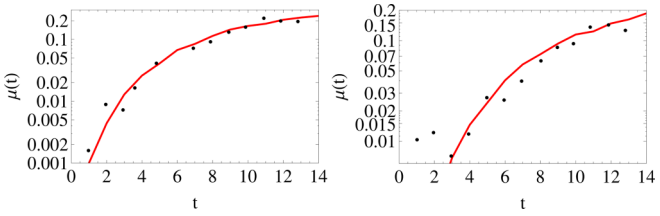

FIG. 4. (Color online) Empiric mortality rates of cars (black dots) fit to present theory (red lines). The data for 1980 Toyota (left) and 1980 Chevrolet (right) from Ref. [3] is fitted with $\{N,\gamma_0,\gamma_1,d\} = \{200,0.023,0.023,0\}$ and $\{200,0.02,0.02,0\}$ respectively. The horizontal axis denotes years.

elevates the initial (infant) mortality rate. Our simulations yield a negative correlation between damage and *increase in* mortality rate; the high initial damage populations age slower than the low initial damage populations to eventually converge to the same μ_0 consistent with Strehler-Mildvan correlation law [39].

The qualitative dependence of average lifetime on damage and repair rate is as intuitively expected [Fig. 6(a)]. When $\gamma_1 = 0$ the average lifespan perfectly fits the curve $\langle\tau\rangle = \beta/\gamma_0$ for both scale-free and random networks. Curiously, when the repair rate exceeds a critical value $\gamma*$ our model allows for immortality. However the weak dependence of τ on $\gamma_1 \ll \gamma_1^*$ implies little return for an increasingly large cost, suggesting why biological immortality is uncommon.

We intuitively expect the onset of death to differ drastically from the early aging process (referred to as disease). This difference will be reflected in the distribution of the number of living nodes that die in a particular time step $[\Delta\phi = \phi(t) - \phi(t-1)]$. In order to tell whether death is just the last disease or a qualitatively different phenomenon, we analyze the distribution $S(\Delta\phi)$ of event sizes before, after, and of the largest drop and notice that the latter is qualitatively as well as quantitatively very different from the former two. Death and disease occupy an entirely different region of the event spectrum [Fig. 6(b)]. What is even more remarkable is that the disease distribution for both evolutionary schemes RN and SFN are quantitatively similar over a wide range of $\Delta\phi$, and obey a power law $S(\Delta\phi) \sim 1/\Delta\phi^{2.7}$ [Fig. 6(c)]. We do not have an explanation for this striking similarity, nor the value of the critical exponent.

We have seen that varying model parameters one at a time produces distinct changes to the mortality curves (Figs. 3 and 5). However we cautiously note that although the model parameters uniquely determine $\mu(t)$, the converse is not true; i.e., species with different attributes can have similar aging curves. To quantitatively establish the degree of uniqueness of $\mu(t)$ we isolate four defining characteristics (initial slope, the plateau value μ_0, average life span τ, and crossover time from an aging to nonaging regime) and see what combination of parameters produce similar characteristics (see Ref. [40] and Appendix).

IV. ANALYTIC THEORY

We now aim to obtain the values of initial decay rates $\langle a\rangle\gamma_0$, the critical vitality ϕ_c, and understand why dependency

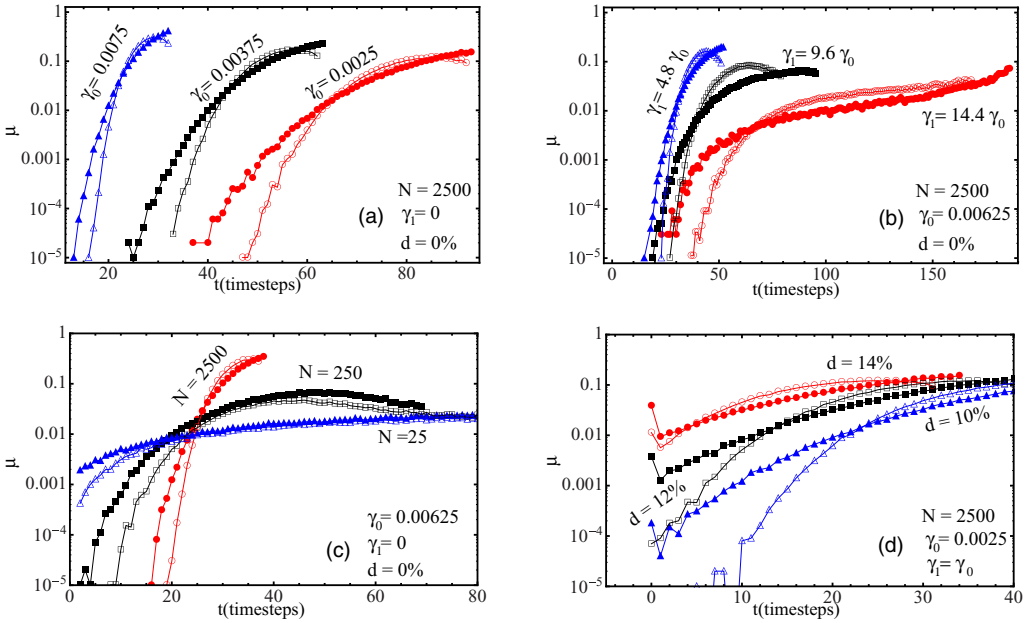

FIG. 5. (Color online) Mortality rate $\mu(t) = -\partial_t s/s$ as a function of time. In each panel we test the effect of one single parameter, keeping the others constant. While random networks (open markers) seem to age slightly faster compared to scale-free networks (filled markers), network topology does not seem to have a significant effect on the qualitative features of μ, in line with experimentally observed universality of mortality curves of different species. We average over 100 networks with 1000 simulations each; thus the lowest probability event we can resolve is of the order $\sim 10^{-5}$, and fluctuations on that order are likely noise. (a) A higher damage probability γ_0 shifts the life-span distribution and mortality curve to the right (b) Repair rate changes the plateau value μ_0 (c) Increasing N increases the slope of μ in the aging (Gompertz) regime. Only for large, complex networks do we find μ varying significantly with t; the simpler the organism the less it ages. (d) The initial damage causes a high infant mortality, but the damage is efficiently repaired soon after birth.

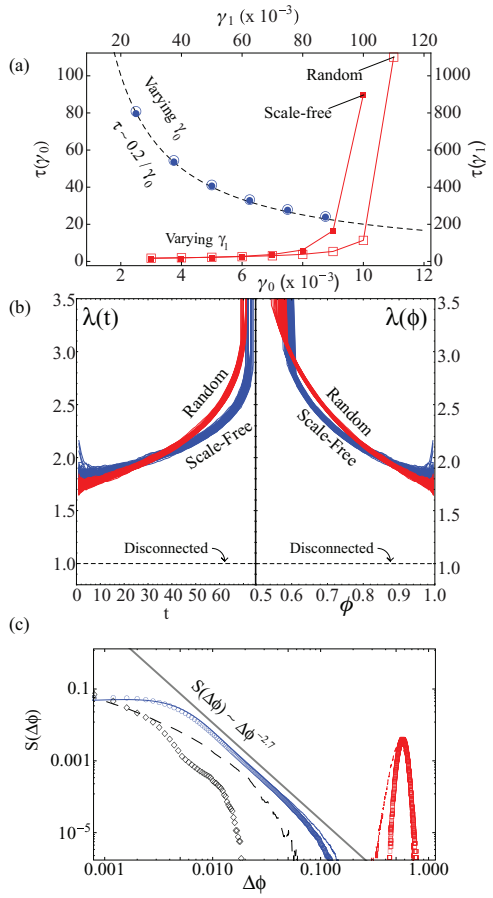

FIG. 6. (Color online) Lifetime, interdependence, and event distribution. (a) Average lifetime $\langle\tau\rangle$ versus damage rate γ_0 (blue circles) and repair rate γ_1 (red squares) for scale-free networks (filled markers) and random networks (open markers) with $N = 2500$. Dashed lines mark $\tau = 0.20/\gamma_0$ for both random and scale-free networks. $\gamma_0 = 0.0065$ is kept constant for both red curves. There seems to be a critical repair rate γ^* for which expected lifespan diverges. Note the remarkable independence of the curves with respect to network structure. (b) $\lambda(t) = \log[\phi(t)]/\gamma_0 t$ as a function of t (left) and ϕ (right) for 100 trajectories on the scale-free (blue) and random (red) networks with $N = 10^6$ pictured in Fig. 1 ($\gamma_1 = 0$). The interdependence parameter λ varies strongly with both t and ϕ, and roughly doubles as more damage is accumulated, until the sudden collapse depicted in Fig. 1 leads to a diverging interdependence. Scale-free networks show a relatively large variation in λ for short times, but rapidly converge on a monotonic increase as the network accumulates damage. Interestingly, scale-free networks begin with a larger value of λ, but random networks become more interdependent rapidly. The interdependence of a set of disconnected nodes (completely independent) have $\lambda_0 = 1$ shown in the dashed line. (c) Probability S that ϕ drops by $\Delta\phi$ for scale-free (open markers) and random (dashed and solid curves) networks. We analyze the distribution of events before the catastrophic failure (blue circles and blue solid curve) of the catastrophic failure itself (red squares and red short dashes) and events after the catastrophic failure, if there are any (black diamonds and black long dashes). Note that different network topologies show remarkable similarity. The largest drop distribution of both random and scale-free networks obey a power law with exponent -2.7, (thick gray line marks slope). Note that the disease (blue) distribution is qualitatively different from death (red). Simulation parameters are $\{N,\gamma_0,\gamma_1,d\} = \{2500,0.0025,0,0\}$.

networks collapse suddenly. On the way, we also hope to understand why these quantities are so similar for both scale-free and random networks, and determine the origin of the Gompertz-like law.

When the system is far from collapse, the probability that two providers of a single node dying at once $\mathcal{O}[\gamma_0^2]$ is negligible compared to that of a single provider dying $\mathcal{O}[\gamma_0]$. Then the total probability p_0 that a node dies is γ_0 plus the probability that the last vital provider of a node dies. If $m(\phi)$ is the probability that a node is left with one last vital provider, we can self-consistently evaluate p_0

$$p_0 = \gamma_0 + m(\phi)p_0(1-\gamma_0). \tag{2}$$

In a single step associated with the aging of the network, the probability that a node is repaired is $p_1 = h(\phi)\gamma_1$, where $h(\phi)$ is the probability that a node has at least the minimum number of providers required to function. Then, the change in the fraction of nodes that are alive is given by

$$\begin{aligned}\Delta\phi &= p_0\phi - p_1(1-\phi)\\ &= -\frac{\gamma_0\phi}{1-m(\phi)(1-\gamma_0)} + \gamma_1 h(\phi)(1-\phi),\end{aligned} \tag{3}$$

where we have used the expression for p_0 as obtained from (2). From (3), we see the origin of the catastrophic (and universal) nature of death. For any arbitrary fully connected network and monotonically decreasing $\phi(t)$, the vital fraction $m(\phi)$ must always start from a finite value in the domain $[0,1]$ and increases towards unity as ϕ decreases, inevitably to cause the first term to dominate the second ($\gamma_0 \ll 1$), and thus leading to a sudden drop in the expected vitality. This is true in general, although the detailed form of the evolution of ϕ depends on the fraction $m(\phi)$ of vital providers and repairable fraction $h(\phi)$ that will vary for different network structures. It is very interesting however, that γ_0 is the same for the reference curve and all overlapping curves, indicating that the somatic damage rate γ_0 *can* be uniquely determined from an experimental μ curve without knowing any of the other parameters describing the system. Equation (3) also indicates an asymptote in longevity for large repair rates, as seen in Fig. 6(a). If we set $\Delta\phi = 0$, we find that the system lives indefinitely when the repair rate γ_1 is set to

$$\gamma_1^* = \frac{\gamma_0\phi^*}{h(\phi^*)(1-\phi^*)[1-m(\phi^*)(1-\gamma_0)]}$$

for any given $\phi^* \in [\phi_c,1]$, i.e., for a vitality larger than the critical vitality ϕ_c. In this case the system damage increases while the vitality decreases until it reaches $\phi = \phi^*$, but maintains that damage (level of connectivity) forever. Of course, (3) governs the *expectation value* of $\phi(t)$, which is the actual value only in the thermodynamic limit $N \to \infty$; any finite-size system will die at least with probability $\gamma_0^{N(\phi(t)-\phi_c)}$ due to statistical fluctuations.

In general, it is a nontrivial task to obtain the exact forms of $m(\phi)$ and $h(\phi)$ and thence the average lifetime, the critical damage fraction, etc. However we can obtain the initial slope $\langle a\rangle\gamma_0 = p_0|_{t=0}$ with which the vitality decreases, and the critical vitality ϕ_c at which the whole system collapses (see dashed lines in Fig. 1) for the case $\gamma_1 = 0$: Let the probability that a node with k providers die be $\sigma^{(k)}$. Then

we can recursively obtain $\sigma^{(1)}$ in terms of the others [41],

$$\sigma^{(1)} = \gamma_0 + P(1,1)\sigma^{(1)} + P(1,2)\sigma^{(2)} + P(1,3)\sigma^{(3)} + \cdots, \tag{4}$$

where $P(1,i)$ is the probability that a node is provided by one other node, and that the provider itself has i providers. The first term corresponds to the probability that a node dies independent of its connectivity.

Since we neglect probabilities of order $\mathcal{O}[\gamma_0^2]$, initially only degree-1 nodes can be killed by the death of their providers. Thus substituting $\sigma^{(k)} = \gamma_0$ for all k apart from $k = 1$, and using $\sum_i P(1,i) = P(1)$ we can obtain from (4) the initial probability that a degree-1 node dies,

$$\sigma^{(1)} = \frac{(2 - P(1,1))\gamma_0}{1 - P(1,1)}. \tag{5}$$

To find the expectation value of the initial slope we must average over the damage rate of all degrees, including $\sigma^{(k)} = \gamma_0$ for $k > 1$

$$\langle a\rangle\gamma_0 = \sum_k P(k)\sigma^{(k)}\Big|_{t=0} = \gamma_0\left(1 + \frac{P(1)}{1 - P(1,1)}\right). \tag{6}$$

Upon substituting the numerical values of $P(1)$ and $P(1,1)$ for the networks we evolved, we obtain $\langle a\rangle = 1.75$ for the neutral scheme and $\langle a\rangle = 1.80$ for non-neutral scheme, i.e., only a $\sim$2.8% difference between two topologies. These initial slopes are consistent with our aging simulations (Fig. 1).

To heuristically estimate the critical vitality ϕ_c, we suppose that there exists a unique value of ϕ_c regardless of the history of the network. If so, then the collapse can occur not only if ϕ approaches ϕ_c in τ steps, it can also occur in precisely one step due to a larger damage, $\gamma_{0c} = 1 - \phi_c$. Thus if we substitute $\gamma_0 \to 1 - \phi_c$ in (4) and let $\sigma^{(i)} \to 1$ for all i to obtain a simple but interesting result,

$$\phi_c = P(1).$$

For the networks we evolved, $P(1)$ is 0.5 for the neutral scheme and 0.6 for the non-neutral scheme. These values are consistent with the critical vitalities we observed in our aging simulations (Fig. 1).

Having estimated the average damage rate and the critical vitality of the network, we now consider the nature of life-span distributions. The probability of network survival $s(t)$ is equal to the probability of $\delta\phi$ being not greater than $\phi - \phi_c$. Since each node dies with probability p_0,

$$\begin{aligned} s(t) &= 1 - \mathrm{Prob}(\Delta\phi > \phi - \phi_c) \\ &= 1 - \sum_{k=0}^{N\phi_c} \binom{N\phi}{N(\phi-\phi_c)+k} p_0^{N(\phi-\phi_c)+k}(1-p_0)^{N\phi_c - k}. \end{aligned} \tag{7}$$

Since $1.75\gamma_0 < p_0 < 1$ is a constant, in the limit $N \to \infty$ the probability of death $1 - s(t)$ simply becomes a unit step function. On the other hand for finite N, the step function softens, and we empirically interpret the rapid transition from $s = 1$ to $s = 0$ as aging. We see that by passing from finite size to infinite size, we also pass from the stochastic to deterministic, and from gradual slow aging to instant aging.

Finally, we consider the sharpness of the transition from $s = 1$ to $s = 0$ to see if there is any relation between our results and the classical Gompertz law for mortality. An approximate evaluation of (7) is carried out and plotted in the Appendix.

V. DISCUSSION

We have built on a similarity between large networks and complex organisms (and machines) to create a minimal model for how large networks (and thence organisms or machines) might age. It is thus important to be self-critical here by comparing our study both with reality and with previous attempts. Any theory that aims to account for a phenomenon as universal as aging, spanning both animate and inanimate objects, needs to be robust, i.e., it should not have such strong assumptions and results that sensitively depend on it. The weak sensitivity of our outcomes to the details of biologically justifiable dependency network structures (Figs. 1–6) seems to satisfy this requirement.

Our analysis differs significantly from earlier theoretical investigations of network failure [29–32] in which nodes are simply removed one by one (systematically or randomly) until networks get fragmented. In these approaches the nodes do not influence the performance of one other, and are not allowed to be repaired. Curiously, the lack of interactions in these models leads to fundamentally different fragmentation dynamics in scale-free and random networks. In contrast, the survival curves we observe are remarkably independent of the network topology (cf. Figs. 1, 5, and 6). The strong interactions between components may indeed be the reason behind the strong similarity of mortality curves among so many organisms. Indeed, this is also consistent with a class of models that do account for strong interactions, though very differently than ours, and have been proposed to explain electrical gird failures [32]. Much still remains to be done in understanding how the form of these interactions leads to differences or similarities in the dynamics.

Our study has focused on the dynamics of networks that age as a consequence of increasing interdependency, and thus leads naturally to the question of how this might be controlled. Since the repair rate, and perhaps the damage rate (to a lesser extent) are experimentally controllable, one might ask if it is possible to vary their temporal character while keeping their average constant. Are there optimal strategies for repair—either in the time domain or in space (i.e., looking at nodes with varying connectivity)? For example, Fig. 6(a) shows that if the system is repaired uniformly, the degree of repair does not make a significant difference for $\gamma_1 < \gamma_1^*$. It would be very useful to know if and how a (temporal or spatial) nonuniform repair strategy improves life span. In networks that are dynamically heterogeneous, we may ask what would be the consequences of differential damage and repair in a network with highly variable turnover, e.g., a network with tissues like the skin or gut that have high damage and repair rates, and the brain which has a low damage and repair rate? At the level of ecologies and colonies, we might ask how does the aging dynamics of a dependency network change when a system consists of parts with aging rates comparable to that of the whole system? We hope that our minimal model may be used to study some of these questions.

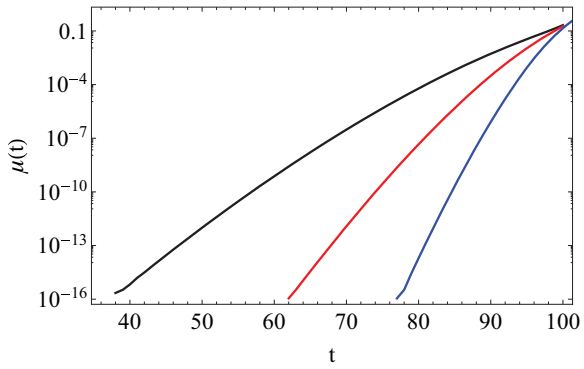

FIG. 7. (Color online) Mortality vs time obtained from (7) for $\phi \ll \phi_c$, $\gamma_0 = 0.0025$ and $N = 50$ (black, left) 100 (red, middle), and 200 (blue, right) is in good qualitative agreement with our simulations and the empiric Gompertz law, which states that $\log \mu(t)$ increases linearly with t early in life.

ACKNOWLEDGMENTS

D.C.V. thanks Anthony J. Leggett for his support, and thanks Pinar Zorlutuna for many stimulating discussions. This work was partly supported by NSF Grants No. NSF-DMR-03-50842, and No. NSF-DMR09-06921, the Wyss Institute for Biologically Inspired Engineering, the Harvard Kavli Institute for Bio-nano Science and Technology, and the MacArthur Foundation.

APPENDIX

Here we discuss various technical points surrounding theory, simulations, and fits.

(i) In order to recover the Gompertz Law analytically, we substitute $\phi(t) \approx e^{-a\gamma_0 t}$ for $t \ll \tau$ in (7) and plot $\mu(t) = -(ds(t)/dt)/s(t)$ in Fig. 7. By approximating the random variables $\phi(t)$ and p_0 by their average value we sharpen the lifetime distributions and hence steepen the mortality curve; however the qualitative features of $\mu(t)$ is recovered.

(ii) We have defined death as the time τ at which ϕ reaches a threshold value 1%, which may seem arbitrary. In order to determine how sensitive our results are to the choice of threshold η, we have analyzed the lifetimes of both network topologies as a function η. For a network as small as $N = 2500$ the value of η changes the lifetime less than 1% for a SFN and less than 12 for a RN (Fig. 8). We find that η dependence rapidly vanishes with increasing N for both network types and conclude that the precise value of η is not important.

(iii) An empirical analysis of historical human mortality data has shown that the value of $\mu(t_0)$ at age t_0 correlates very strongly with $\mu(t_1)$ at age t_1 for a wide variety of societies and historical periods [42]. In other words, for an arbitrary collection of people (presumably with different damage and/or repair rates and initial conditions), the mortality rate at any two ages are correlated, with correlation coefficient $\rho \sim 1$. To test whether our model yields this behavior, we plot the number of deaths within t_0 and $t_0 + 5$ against that within t_1 and $t_1 + 5$ for a range of γ_0, γ_1, d and network types (see Fig. 9). The bin size was chosen as 5 instead of 1 in order to reduce statistical error (e.g., commonly less than 10^{-6} of the networks die exactly at $t = 1$). We observe that our model does yield a very high correlation between μ pairs for a wide range of network parameters and network types, although the trend becomes less pronounced for wider intervals of $t_0, t1$. Specifically, we find a correlation of $\rho \sim 0.8, 0.98$, and 0.99 for $\{t_0, t_1\} = \{0,20\}, \{10,20\}$, and $\{15,20\}$ respectively. These correlation values are nearly identical for scale-free and random networks and are in qualitative accordance with empiric observation.

(iv) To determine whether model parameters $\{N, \gamma_0, \gamma_1, d\}$ can be determined uniquely given experimental $\mu(t)$ data we performed simulations sweeping the parameter space

$$N \in 50,100,250,500,700,800,900,1000,1500,2000,$$
$$\gamma_0 \in 2,4,6,8,10,15,20,25,30,35 \times 10^{-3},$$
$$\gamma_1 \in 1,2,\ldots,10 \times \gamma_0, \quad d \in 0,0.5,\ldots,10 \text{ (percent)}$$

and checked if non-neighboring parameters give more similar $\mu(t)$ curves than neighboring ones (cf. below for details). For each set of parameters we generated 12 networks upon which

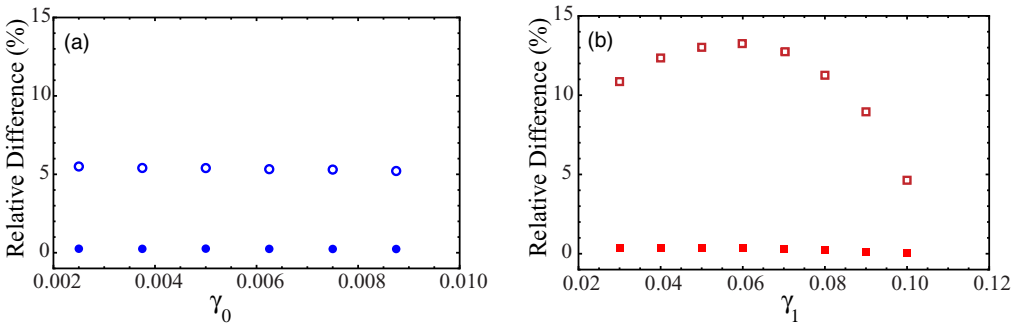

FIG. 8. (Color online) Sensitivity of outcomes to the definition of death. (a) The percent lifetime difference between choices $\eta = 1\%$ and 50% for scale-free (filled circles) and random (empty circles) dependence networks, with varying γ_0 and $\gamma_1 = 0$. There is a fairly constant 5% difference independent of γ_0 for random networks, and below 1% for scale-free networks. (b) The percent lifetime difference between choices $\eta = 1\%$ and 50% for varying γ_1, with $\gamma_0 = 0.00625$. Scale-free networks continue to have below 1% difference between the two threshold choices, while the variation is more significant for random networks with large repair rate γ_1. The relative difference decreases if the two thresholds η are closer to one another. For both graphs $N = 2500$, $d = 0$.

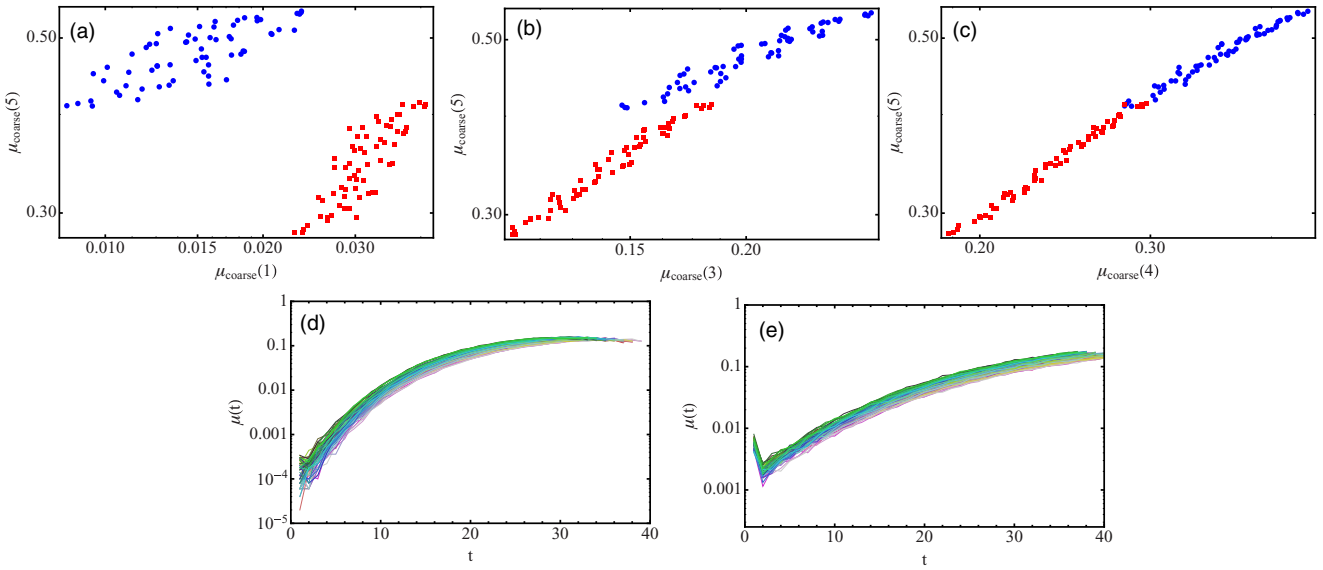

FIG. 9. (Color online) Testing for universality in mortality patterns. Dependence of old age mortality $\mu(5) = \text{Prob}(20 < \tau < 25)$ on younger age mortality $\mu(i) = \text{Prob}(5i - 5 < \tau < 5i)$ for $i = 1$ (a), 3 (b), 4 (c) for a range of network types (RN blue circles, SFN red squares) and system parameters, $\gamma_0 = \{0.0026, 0.0027, 0.0028, 0.0029\}$, $\gamma_1 = \{0.0026, 0.0027, 0.0028, 0.0029\}$, $d = \{12.1, 12.2, 12.3, 12.4\}$ (τ is the time of death). The mortality curves generated by this range of parameters is displayed for RN (d) and SFN (e). While the universal (yet species-specific) trend observed in Ref. [42] between $\mu(i)$ and $\mu(i + j)$ (for fixed j) is qualitatively present in our model, the trend vanishes for large enough j.

3000 simulations were performed, providing a reasonable level of confidence in the statistical accuracy of the simulations. To quantitatively compare the simulation results, $\mu(t)$ is broken into four averaged characteristics: The initial slope, the saturation point, the crossover time between the initial growth and saturation, and the observed lifetime [see Fig. 10(a)]. The threshold for similarity of the curve characteristics is determined by averaging over the differences in nearest neighbors in the $(N, \gamma_0, \gamma_1, d)$ parameter space (i.e., the $\sum_{k=1}^{8} |\tau_{\text{ref}} - \tau_{S_k}|$, with the parameters in the simulation S_k being different from the reference simulation in only one position, and a nearest neighbor). Thus, simulation outcomes are considered similar to a reference if they are not nearest neighbors (in parameter space) with the reference, and if the differences in all four characteristics simultaneously fall within the threshold variation. Figure 10(b) shows one such overlapping curve with $d = 4.5$, $N = 700$, and $\gamma_1 = 5\gamma_0$ (compared to $d = 0\%$, $N = 250$, and $\gamma_1 = 0$ for the reference simulation in black). The inset of Fig. 10(b) shows all 214 simulation parameters that yields mortality curves considered similar to the reference curve (about 0.9% of all of the simulated parameters), and shows that a rather wide range of parameters may give qualitatively

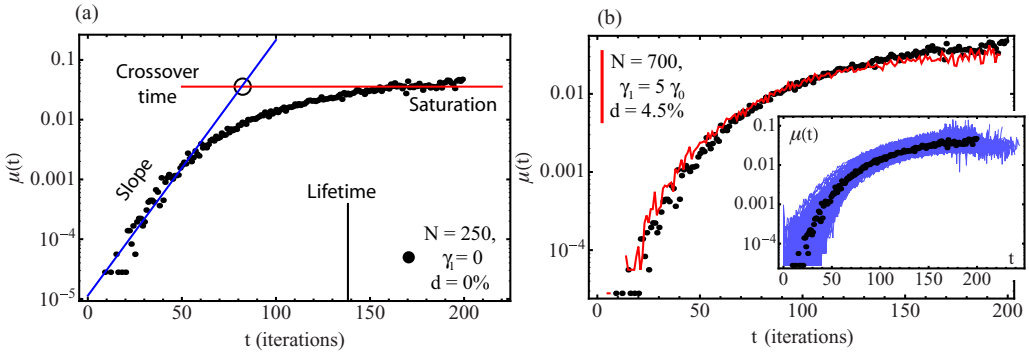

FIG. 10. (Color online) Uniqueness of $\mu(t)$ as determined by initial slope, saturation value crossover time, and average lifetime. (a) A simulation is quantified in terms of four parameters: The initial slope, the final saturation value, the crossover time, and the lifetime. Shown is a reference simulation with $N = 250$, $\gamma_0 = 0.002$, $\gamma_1 = 0$, and $d = 0\%$ (b) The nonuniqueness of $\mu(t)$ as the parameters are varied. In the main panel and the inset, the black points correspond to the reference simulation in (a). The three red line in the main panel has $N = 700$, $\gamma_0 = 0.002$, $\gamma_1 = 5\gamma_0$, and $d = 4.5\%$. The average lifetime for the red curve is $\tau = 133$, within 4.3% of the lifetime of the reference curve. There is moderate variation between the curves for small and large t, but it would be difficult to unambiguously differentiate between the two sets of parameters when fitting experimental data. The inset shows the same reference simulation (black points), along with all 214 sets of simulated parameters that satisfy the threshold criterion. Each blue line has $250 \leqslant N \leqslant 2000, 0 \leqslant \gamma_1/\gamma_0 \leqslant 9$, and $0 \leqslant d \leqslant 8.5$, all with $\gamma_0 = 0.002$.

similar behavior in μ and τ (with the latter not shown). It is interesting to note that γ_0 is the same for the reference curve and all overlapping curves, indicating that an empirically observed death rate γ_0 may be uniquely determined.

[1] S. Horiuchi, Pop. Dev. Rev. **29**, 127 (2003).
[2] G. Caughley, Ecology **47**, 906 (1966).
[3] J. W. Vaupel, J. R. Carey, K. Christensen, T. E. Johnson, A. I. Yashin *et al*., Science **280**, 855 (1998).
[4] K. A. Highes and R. M. Raynolds, Ann. Rev. Entomol. **50**, 421 (2005).
[5] B. T. Weinert and P. S. Timiras, J. Appl. Physiol. **95**, 1706 (2003).
[6] E. H. Blackburn, Nature (London) **408**, 53 (2000).
[7] D. Harman, J. Gerontol. **2**, 298 (1957).
[8] A. Baudisch, Gerontology **58**, 481 (2012).
[9] P. B. Medawar, *An unsolved problem in biology* (H. K. Lewis & Co., London, 1952).
[10] G. C. Williams, Evolution **11**, 398 (1957).
[11] W. D. Hamilton, J. Theor. Biol. **12**, 12 (1966).
[12] P. B. Medawar, Mod. Quart. **1**, 30 (1946).
[13] M. R. Rose, *Evolutionary Biology of Aging* (Oxford University Press, New York, 1991).
[14] T. B. L. Kirkwood, Mech. Aging Dev. **123**, 737 (2002).
[15] T. B. L. Kirkwood, Nature (London) **270**, 301 (1977).
[16] P. A. Abrams and D. Ludwig, Evolution **49**, 1055 (1995).
[17] J. W. Curtsinger, H. H. Fukui, D. R. Townsend, and J. W. Vaupel, Science **258**, 461 (1992).
[18] J. R. Carey, P. Liedo, D. Orozco, and J. W. Vaupel, Science **258**, 457 (1992).
[19] D. E. L. Promislow, M. Tatar, A. A. Khazaeli, and J. W. Curtsinger, Genetics **143**, 839 (1996).
[20] D. A. Gray and W. H. Cade, Can. J. Zool. **78**, 140 (2000).
[21] R. A. Miller, R. Dysko, C. Chrisp, R. Seguin, L. Linsalata *et al*., J. Zool. **250**, 95 (2000).
[22] R. A. Miller, J. M. Harper, R. C. Dysko, S. J. Durkee, and S. N. Austad, Exp. Biol. Med. **227**, 500 (2002).
[23] D. Reznick, G. Buckwalter, J. Groff, and D. Elder, Exp. Gerontol. **36**, 791 (2001).
[24] M. W. Gray, J. Lukes, J. M. Archibald, P. J. Keeling, and W. Doolittle, Science **330**, 920 (2010).
[25] M. Lynch, Proc. Natl. Acad. Sci. USA **104**, 8597 (2007).
[26] A. Stoltzfus, J. Mol. Evol. **49**, 169 (1999).
[27] H. J. M. Kiss, Á. Mihalik, T. Nánási, B. Öry, Z. Spiró, C. Söti, and P. Csermely, BioEssays **31**, 651 (2009).
[28] M. Scheffer, J. Bascompte, W. A. Brock, V. Brokvin, S. R. Carpenter *et al*., Nature (London) **461**, 53 (2009).
[29] R. Albert, H. Jeong, and A. L. Barabasi, Nature (London) **406**, 378 (2000).
[30] T. Tanizawa, G. Paul, R. Cohen, S. Havlin, and H. E. Stanley, Phys. Rev. E **71**, 047101 (2005).
[31] R. Cohen, D. ben-Avraham, and S. Havlin, Phys. Rev. E **66**, 036113 (2002).
[32] S. V. Buldyrev, R. Parshani, G. Paul, H. E. Stanley, and S. Havlin, Nature (London) **464**, 1025 (2010).
[33] G. I. Simkó, D. Gyurkó, D. V. Veres, T. Nánási, and P. Csermely, Genome Med. **1**, 90 (2009).
[34] L. A. Gavrilov and N. S. Gavrilova, J. Theor. Biol. **213**, 527 (2001).
[35] R. A. Laird and T. N. Sherratt, J. Evol. Biol. **22**, 974 (2009).
[36] H. Jeong, B. Tombor, R. Albert, Z. N. Oltvai, and A. L. Barabasi, Nature (London) **407**, 651 (2000).
[37] For two other choices (τ_0, the time at which no nodes are left alive, or τ_m, the time at which the largest drop in ϕ occurs), we have $\tau_0 \approx \tau_m \approx \tau$ for large N. We find that in smaller networks (particularly RN) these times may differ. Interestingly τ is not always well defined in nature either; for example, parts of cockroaches are known to survive for weeks after the insect is decapitated [43].
[38] In order to determine how sensitive our results are to the choice of threshold η, we have analyzed the lifetimes of both network topologies as a function η. For a network as small as $N = 2500$, the choice of η changes the lifetime by $\sim$1% for a SFN and $\sim$%10 for a RN. We find that for $N > \mathcal{O}[10^6]$ the η dependence practically vanishes for both network types. We therefore conclude that the precise value of η is not important.
[39] B. L. Strehler and A. S. Mildvan, Science **132**, 14 (1960).
[40] The threshold for similarity of the curve characteristics is determined by averaging over the differences in nearest neighbors in the (N,γ_0,γ_1,d) parameter space (i.e., the $\sum_{k=1}^{8} |\tau_{\rm ref} - \tau_{S_k}|$, with the parameters in the simulation S_k being different from the reference simulation in only one position, and a nearest neighbor). Thus, simulation outcomes are considered similar to a reference if they are not nearest neighbors (in parameter space) with the reference, and if the differences in all four characteristics simultaneously fall within the threshold variation.
[41] Analogous equations can be written for $\sigma^{(i)}$ for $i > 1$; however these equations will depend on $P(i; x_1 x_2 \ldots x_i)$, the probability that a node with i providers has one provider with x_1 providers, one provider with x_2 providers, and so on. Fortunately we do not need these equations to obtain ϕ_c and a.
[42] M. Ya. Azbel, Phys. Rev. E **66**, 016107 (2002).
[43] C. Q. Choi, Sci. Am. **297**, 116 (2007).